

Standard Gibbs' energies of formation of BaCuO₂, Y₂Cu₂O₅ and Y₂BaCuO₅

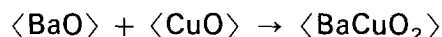
A. M. AZAD, O. M. SREEDHARAN

Metallurgy Division, Indira Gandhi Centre for Atomic Research, Kalpakkam 603 102, Tamil Nadu, India

K. T. JACOB

Department of Metallurgy, Indian Institute of Science, Bangalore 560 012, India

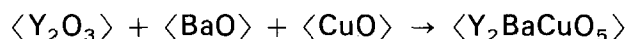
The Gibbs' energies of formation of BaCuO₂, Y₂Cu₂O₅ and Y₂BaCuO₅ from component oxides have been measured using solid state galvanic cells incorporating CaF₂ as the solid electrolyte under pure oxygen at a pressure of 1.01 × 10⁵ Pa



$$\Delta G_{f,ox}^{\circ} (\pm 0.3) \text{ (kJ mol}^{-1}\text{)} = -63.4 - 0.0525 T \text{ (K)}$$



$$\Delta G_{f,ox}^{\circ} (\pm 0.3) \text{ (kJ mol}^{-1}\text{)} = 18.47 - 0.0219 T \text{ (K)}$$



$$\Delta G_{f,ox}^{\circ} (\pm 0.7) \text{ (kJ mol}^{-1}\text{)} = -72.5 - 0.0793 T \text{ (K)}$$

Because the superconducting compound YBa₂Cu₃O_{7-δ} coexists with any two of the phases CuO, BaCuO₂ and Y₂BaCuO₅, the data on BaCuO₂ and Y₂BaCuO₅ obtained in this study provide the basis for the evaluation of the Gibbs' energy of formation of the 1–2–3 compound at high temperatures.

1. Introduction

Since the discovery of superconductivity in the quarternary ceramic oxide YBa₂Cu₃O_{7-δ}(1–2–3) compound by Wu *et al.* [1] in 1987, systematic studies on thermodynamic characterization of phases in the YO_{1.5}–BaO–CuO system have been reported [2–9]. An isothermal section of the phase diagram of this system in air at 1223 K has been reported by several investigators [10–15]. A representative phase diagram reported recently by Jacob and Waseda [15] is shown in Fig. 1. Although there is a considerable disagreement regarding stable phases in the pseudobinary YO_{1.5}–BaO among the various investigators, there is a general consensus regarding the phases that coexist with the 1–2–3 compound. The 1–2–3 compound has been found to coexist with any two of the phases CuO, BaCuO₂ and Y₂BaCuO₅. Hence for the thermodynamic characterization of 1–2–3 compound, it is necessary to determine the thermodynamic stability of BaCuO₂ and Y₂BaCuO₅. The quarternary oxide Y₂BaCuO₅ has been found to coexist with Y₂Cu₂O₅ and CuO (or Y₂O₃). Therefore, the Gibbs' energy of formation of Y₂Cu₂O₅ is also required for thermodynamic characterization of the 1–2–3 compound.

Pankajavalli and Sreedharan [4] have determined the standard Gibbs' energy of formation of Y₂Cu₂O₅, in metastable equilibrium with Cu₂O and Y₂O₃, using

an oxide solid electrolyte over the temperature range 1097–1292 K. Their results are in fair agreement with the values reported by Tretyakov *et al.* [16] and more recently by Kale and Jacob [3], both employing a solid state e.m.f. technique. The stability of Y₂BaCuO₅ over the range 717–1021 K has been determined by Pankajavalli and Sreedharan [6] from oxygen potential measurements over the phase mixture Y₂BaCuO₅ + Y₂BaO₄ + Cu₂O. Measurements of Gibbs' energy of formation of BaCuO₂ have not thus far been reported in the literature; this paper reports these measurements for BaCuO₂, Y₂Cu₂O₅ and Y₂BaCuO₅ using solid state cells incorporating CaF₂ as the solid electrolyte. The condensed phase electrodes were equilibrated with pure oxygen at a pressure of 1.01 × 10⁵ Pa.

2. Experimental procedure

2.1. Materials

Reagent grade anhydrous BaCO₃ (purity > 99.5%), Y₂O₃ (purity > 99.99%), CuO (purity > 99.8%) and ZrO₂ (purity > 99.99%) were used as the starting materials. Fluorides of barium and yttrium of purity higher than 99.99% were used. Single crystals of CaF₂, 10 mm diameter and 3–4 mm, thick, were procured.

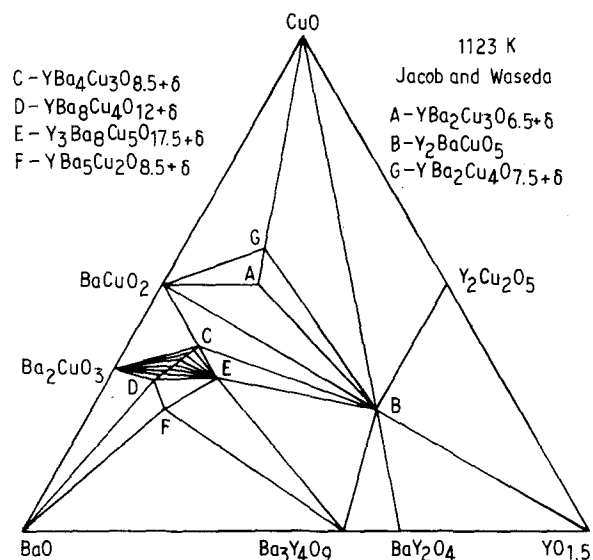


Figure 1 Isothermal section of the $YO_{1.5}$ -BaO-CuO phase diagram at 1123 K.

An intimate mixture of $BaCO_3$ and ZrO_2 in the molar ratio of 2:3 was compacted into cylindrical discs of 10 mm diameter and 3–4 mm thickness under a pressure of 100 MPa. These pellets were calcined in air at 1273 K for 24 h. The pellets were ground into a fine powder and the procedure was repeated two or three times to ensure the completion of the solid-state reaction. The product was identified as a two-phase mixture of $BaZrO_3$ and ZrO_2 by powder X-ray diffraction (XRD). No free BaO or $BaCO_3$ were detected in the final product.

Equimolar two-phase mixtures containing $BaCuO_2 + CuO$, $Y_2Cu_2O_5 + CuO$ and $Y_2BaCuO_5 + CuO$ were prepared by taking appropriate starting materials in the required proportions. A summary of experimental conditions used for the synthesis of oxide mixtures is given in Table I. The electrodes were prepared by mixing the oxide mixtures with the corresponding stable fluorides. The compositions of the electrodes are given in Table II. All the mixtures were individually compacted at a pressure of 100 MPa into cylindrical pellets of 10 mm diameter and 2–3 mm thickness to serve as electrodes.

TABLE I Summary of experimental conditions used for the synthesis of oxide compounds

Starting mixture (molar ratio)	Temperature (K)	Durations of heat treatment (h)	Phases identified after heat treatment by X-ray diffraction
$BaCO_3 + ZrO_2$ (1:2)	1273	24 + 24 ^a	$BaZrO_3 + ZrO_2$
$BaCO_3 + CuO$ (1:2)	(i) 1173 (ii) 1223	24 6	$BaCuO_2 + CuO$
$Y_2O_3 + CuO$ (1:2)	1273	24	$Y_2Cu_2O_5 + CuO$
$Y_2O_3 + BaCO_3 + CuO$ (1:1:2)	1273	36 + 24 ^a	$Y_2BaCuO_5 + CuO$

^a The pellets were ground after 24 h heat treatment, repelletized and heat treated for a further 24 h.

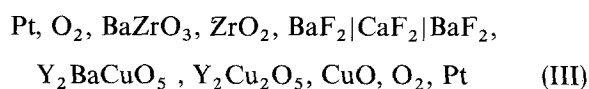
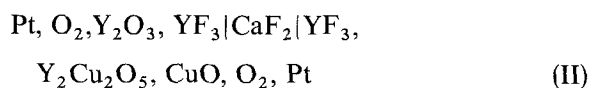
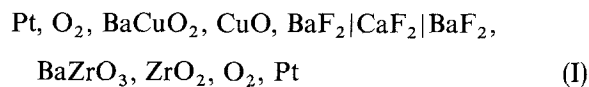
TABLE II Composition of electrodes

Material(s)	Coexisting fluoride	Weight ratio
$BaZrO_3 + ZrO_2$	BaF_2	1:1:1
$BaCuO_2 + CuO$	BaF_2	1:1:1
$Y_2Cu_2O_5 + CuO$	YF_3	1:1:1
$Y_2BaCuO_5 + CuO$ + $Y_2Cu_2O_5$	BaF_2	1:1:1:1
Y_2O_3	YF_3	3:1

2.2. E.m.f. measurements

A stacked-pellet assembly described elsewhere [17] was employed for the e.m.f. measurements. The oxygen potential at the two electrodes was fixed by flowing high-purity oxygen (99.99%) at a flow rate of $1 \text{ dm}^3 \text{ h}^{-1}$ and a pressure of $1.01 \times 10^5 \text{ Pa}$ over them. Prior to admission into the cell, the oxygen was passed through drierite (anhydrous $CaCl_2$) for the removal of traces of moisture present in the cylinder gas. The temperature of the cell was measured using a Pt-Pt/10% Rh thermocouple calibrated against the melting points of Sn, Bi, Zn, Sb and Ag. The head of the galvanic cell assembly was located in the isothermal zone of a non-inductively wound furnace. Temperature of the furnace was regulated by a proportional power controller to better than $\pm 1 \text{ K}$. The reproducibility of the e.m.f. data was verified by thermal cycling and microcoulometric titration. Absence of asymmetric potential was checked by measuring near null e.m.f. with $Y_2O_3 + YF_3$ on either side of the solid electrolyte.

The reversible e.m.f. of the following cells were measured as a function of temperature



The cells are written such that the right-hand electrodes are positive.

In these cells attainment of electrochemical equilibria were found to be rather sluggish and steady e.m.f. was realized only after a few hours. At lower temperatures, it took 8–24 h to establish equilibrium among various coexisting phases at the electrodes. Each of these cells were operated for a period of 7–10 days. In some cases, the discs of CaF_2 solid electrolyte were often found to have become opaque, presumably due to the finite solubility of oxygen in CaF_2 and precipitation of CaO . This opaque layer could, however, be easily removed by polishing the surfaces on the "Corosil" 600 paper until the translucence was regained. After each e.m.f. run, the electrode pellets could be detached effortlessly indicating the absence of any reaction between the electrode and CaF_2 electrolyte.

The e.m.f. of Cells I, II and III are plotted in Figs 2–4. The e.m.f. is a linear function of temperature. The least squares regression analysis gives the following

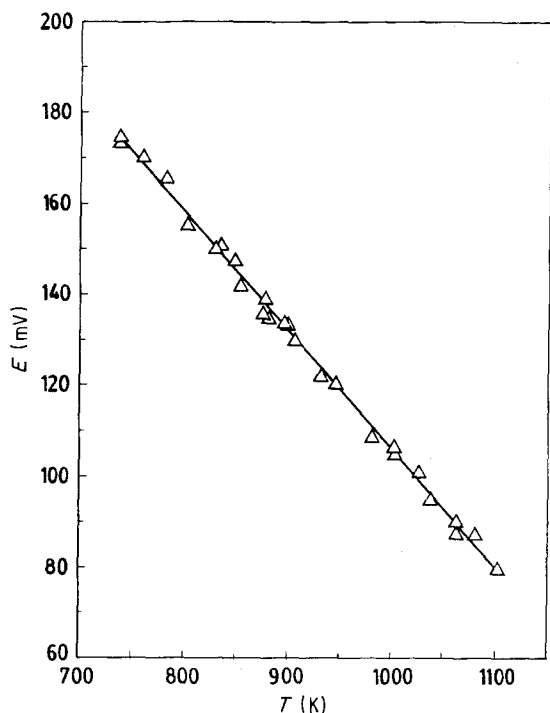


Figure 2 Temperature dependence of e.m.f. of Cell I.

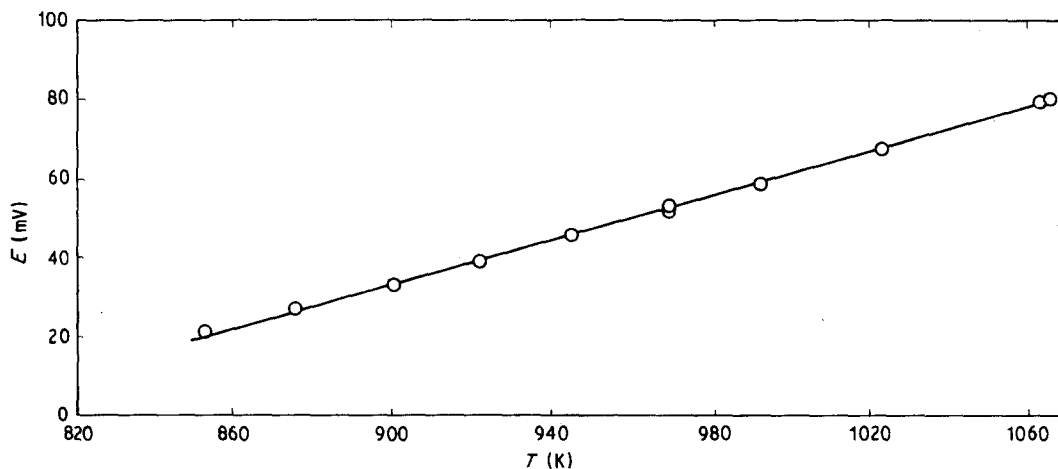


Figure 4 Temperature dependence of e.m.f. of Cell III.

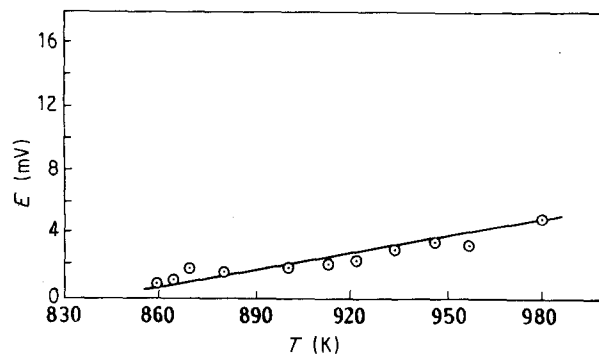


Figure 3 Temperature dependence of e.m.f. of Cell II.

expressions for the e.m.f.

$$E_I(\pm 1.6) \text{ (mV)} = 367.4 - 0.261199 T(\text{K}) \quad (1)$$

in the temperature range 736–1102 K

$$E_{II}(\pm 0.5) \text{ (mV)} = -31.9 + 0.037802 T(\text{K}) \quad (2)$$

in the temperature range 861–980 K,

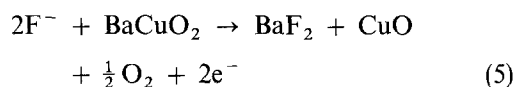
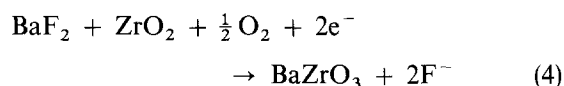
$$E_{III}(\pm 0.9) \text{ (mV)} = -224.8 + 0.286507 T(\text{K}) \quad (3)$$

in the temperature range 853–1066 K.

3. Discussion

3.1. The Gibbs' energy of formation of BaCuO_2

The two half-cell reactions in Cell I are



For the passage of 2 F of electricity, the virtual cell reaction is



The corresponding standard Gibbs' energy change (ΔG_R^0) for Reaction 6, computed from the e.m.f. is

$$\Delta G_R^0(\pm 0.30) \text{ (kJ)} = -70.9 + 0.050405 T(\text{K}) \quad (7)$$

This is related to the standard Gibbs' energies of formation of BaCuO₂ and BaZrO₃ from the constituent binary oxides ($\Delta G_{f,ox}^0$) as

$$\Delta G_R^0 = \Delta G_{f,ox}^0(\text{BaZrO}_3) - \Delta G_{f,ox}^0(\text{BaCuO}_2) \quad (8)$$

Levitskii [18] had reported data for the Gibbs' energy of formation of BaZrO₃

$$\begin{aligned} \Delta G_{f,ox}^0(\text{BaZrO}_3)(\text{kJ mol}^{-1}) &= (-134.3 \pm 6.7) \\ &- (2.1 \pm 4.6) \times 10^{-3} T(\text{K}) \end{aligned} \quad (9)$$

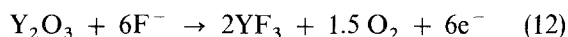
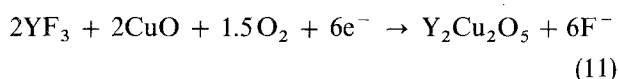
Combining Equations 7–9, the Gibbs' energy of formation of BaCuO₂ from component oxides in the temperature range 736–1102 K is obtained

$$\begin{aligned} \Delta G_{f,ox}^0(\pm 0.3)(\text{kJ mol}^{-1}) \\ = -63.4 - 0.0525 T(\text{K}) \end{aligned} \quad (10)$$

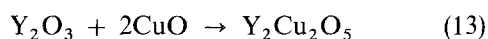
It can be seen from Equation 10 that the entropy change, $\Delta S_{f,ox}^0$ for the solid reaction between BaO and CuO to form BaCuO₂ is rather high (52.5 J K⁻¹ mol⁻¹). The error limit on $\Delta S_{f,ox}^0$ is estimated as ± 10 J K⁻¹ mol⁻¹. The measured values correspond to a composition saturated with respect to CuO. In the absence of reliable information on the defect structure and nonstoichiometry of BaCuO₂, it is not possible at present to explain the high value for the entropy. Moreover, there are no data reported in the literature with which the present values of $\Delta G_{f,ox}^0$ of BaCuO₂ can be compared. Because of the limited temperature range covered in the study, the derived second law entropy is not likely to be very accurate. More accurate data on entropy must await calorimetric studies on BaCuO₂.

3.2. The Gibbs' energy of formation of Y₂Cu₂O₅

The two half-cell reactions in Cell II are



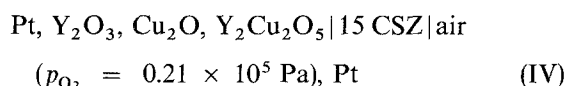
Thus for the passage of 6 F of electricity, the virtual cell reaction corresponding to Cell II is



The standard Gibbs' energy change ($\Delta G_R^0 = -6 F$) for the reaction represented by Equation 13 is identical with the standard Gibbs' energy of formation of Y₂Cu₂O₅ from the constituent oxides. Hence from the e.m.f. of Cell II

$$\Delta G_{f,ox}^0(\pm 0.3)(\text{kJ mol}^{-1}) = 18.47 - 0.0219 T(\text{K}) \quad (14)$$

Tretyakov *et al.* [16], Pankajavalli and Sreedharan [4] carried out e.m.f. measurements on oxide galvanic cells of the following configuration over the ranges 1173–1340 and 1097–1292 K, respectively:



Equations 15 and 16 were derived by Tretyakov *et al.* [16] and Pankajavalli and Sreedharan [4], respectively, for the Gibbs' energy of formation of Y₂Cu₂O₅ from oxides

$$\Delta G_{f,ox}^0(\text{kJ mol}^{-1}) = 21.24 - 0.02281 T(\text{K}) \quad (15)$$

$$\Delta G_{f,ox}^0(\text{kJ mol}^{-1}) = 10.91 - 0.01341 T(\text{K}) \quad (16)$$

Kale and Jacob [3] have proposed a phase diagram for the Cu–Y–O system, according to which Cu₂O, Y₂O₃ and Y₂Cu₂O₅ do not coexist at equilibrium. They have measured the oxygen potential corresponding to the three-phase field YCuO₂ + Y₂Cu₂O₅ + Y₂O₃ by an oxide-c.m.f. method over the range 873–1323 K. The Gibbs' energy of formation of Y₂Cu₂O₅ suggested by Kale and Jacob [3] is

$$\begin{aligned} \Delta G_{f,ox}^0(\pm 0.12)(\text{kJ mol}^{-1}) \\ = 11.21 - 0.01507 T(\text{K}) \end{aligned} \quad (17)$$

Based on the assumption of a regular solution model, for the liquid phase and an incorrect phase diagram, Rao *et al.* [19] derived an expression for the Gibbs' energy of Y₂Cu₂O₅

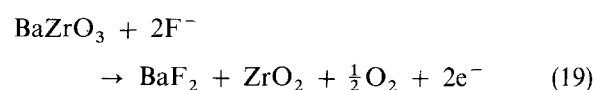
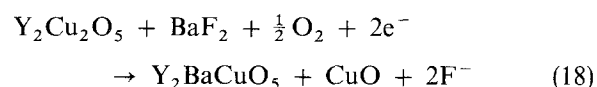
$$\Delta G_{f,ox}^0(\text{kJ mol}^{-1}) = -59.21 + 0.029169 T(\text{K}) \quad (18)$$

These measurements are compared in Fig. 5. The solid segments correspond to the actual temperature range of measurements in each investigation and the extrapolations are shown by broken lines. It can be seen from the figure that except for the estimate reported by Rao *et al.* [19], the other three sets of measurements are in fair agreement with the present investigation. The standard entropy of formation $\Delta S_{f,ox}^0$ for the solid reaction between Y₂O₃ and CuO obtained in this study (21.9 J K⁻¹ mol⁻¹) is in good agreement with that reported by Tretyakov *et al.* (22.8 J K⁻¹ mol⁻¹) and in qualitative agreement with those suggested by Kale and Jacob (15.1 J K⁻¹ mol⁻¹) and Pankajavalli and Sreedharan (13.4 J K⁻¹ mol⁻¹). However, the Gibbs' energies from the four experimental studies agree within ± 1 kJ.

The measured thermodynamic data for Y₂Cu₂O₅ suggest its disproportionation into Y₂O₃ and CuO at lower temperatures. The calculated decomposition temperatures are 931 K from the data of Tretyakov *et al.* [16], 814 K from the data of Pankajavalli and Sreedharan [4] and 744 K from the measurements of Kale and Jacob [3]. Because of the sluggish kinetics associated with the solid state reaction, the decomposition of Y₂Cu₂O₅ is not observed during differential thermal analysis (DTA).

3.3. The Gibbs' energy of formation of Y₂BaCuO₅

The two half-cell reactions in Cell III are



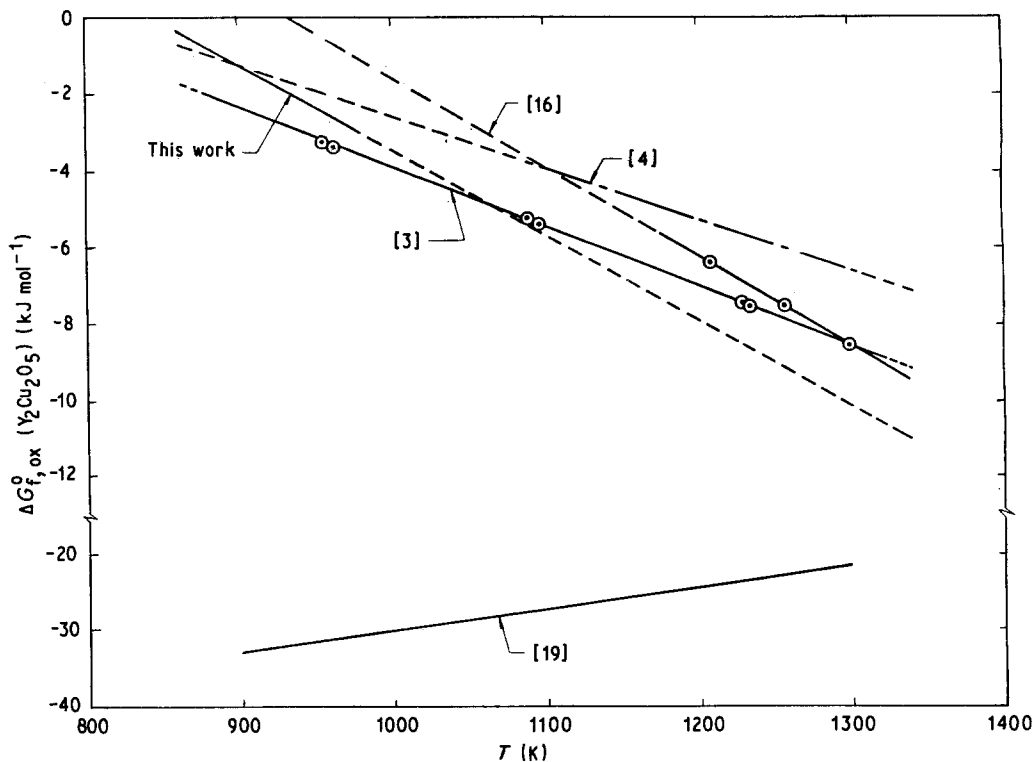
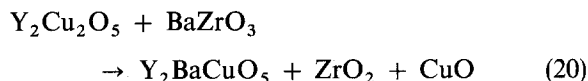


Figure 5 Comparison of $\Delta G_{f,ox}^0$ of $Y_2Cu_2O_5$.

For the passage of 2 F of electricity, the virtual cell reaction is



The Gibbs' energy change associated with this reaction, computed from the e.m.f. is

$$\Delta G_R^0 (\pm 0.17) \text{ (kJ)} = 43.4 - 0.055289 T \text{ (K)} \quad (21)$$

Further, the Gibbs' energy change for the cell reaction can be expressed in terms of Gibbs' energies of formation of Y_2BaCuO_5 , $Y_2Cu_2O_5$ and $BaZrO_3$

$$\Delta G_R^0 = \Delta G_{f,ox}^0(Y_2BaCuO_5) - \Delta G_{f,ox}^0(Y_2Cu_2O_5) - \Delta G_{f,ox}^0(BaZrO_3) \quad (22)$$

Now, there are four independent sets of data (as discussed in Section 3.2) on $\Delta G_{f,ox}^0$ of $Y_2Cu_2O_5$. In order to minimize the systematic errors, Equation 14 from the present study is used to compute the $\Delta G_{f,ox}^0$ of Y_2BaCuO_5 . By combining Equation 22 with Equations 9, 14 and 21, an expression for Gibbs' energy of formation of Y_2BaCuO_5 from the component oxides Y_2O_3 , BaO and CuO is obtained

$$\Delta G_{f,ox}^0 (\pm 0.7) \text{ (kJ mol}^{-1}\text{)} = -72.5 - 0.0793 T \text{ (K)} \quad (23)$$

in the temperature range 853–1066 K.

The only other report on the Gibbs' energy of formation of Y_2BaCuO_5 is by Pankajavalli and Sreedharan [6] who measured the oxygen potential corresponding to the three-phase mixture $Y_2BaCuO_5 + Y_2BaO_4 + Cu_2O$ in the temperature interval from 717–1021 K. The values of $-130.6 \text{ kJ mol}^{-1}$ at 850 K

and $-125.4 \text{ kJ mol}^{-1}$ at 1050 K for $\Delta G_{f,ox}^0$ of Y_2BaCuO_5 from the work of Pankajavalli and Sreedharan [6] are in poor agreement with -139.9 and $-155.7 \text{ kJ mol}^{-1}$ at the respective temperatures obtained in the present investigation. The positive value of $79.3 \text{ J K}^{-1} \text{ mol}^{-1}$ for $\Delta S_{f,ox}^0$ obtained in this work contrasts with the negative value of $-20 \text{ J K}^{-1} \text{ mol}^{-1}$ suggested by Pankajavalli and Sreedharan [6].

4. Conclusion

The standard Gibbs' energies of formation of the compounds $BaCuO_2$, $Y_2Cu_2O_5$ and Y_2BaCuO_5 from component oxides were determined from the reversible e.m.f. of solid state cells based on CaF_2 under pure oxygen at a pressure of $1.01 \times 10^5 \text{ Pa}$. These data provide a basis for evaluating the thermodynamic stability of 1–2–3 compound under identical conditions.

Acknowledgements

The authors thank Shri C. V. Sundaram, Director, IGCAR, Dr Placid Rodriguez, Head, Metallurgy and Materials Programme, and Shri J. B. Gnanamoorthy, Head, Metallurgy Division, for their keen interest and constant encouragement during this collaborative effort.

References

1. M. K. WU, J. R. ASHBURN, C. J. TORNG, P. H. HOR, R. L. MENG, L. GAO, Z. J. HUANG, Y. Q. WANG and C. W. CHU, *Phys. Rev. Lett.* **58** (1987) 908.
2. G. M. KALE and K. T. JACOB, *Solid State Ionics*. **34** (1989) 247.
3. *Idem.*, *Mater. Chem.* **1** (1989) 515.

4. R. PANKAJAVALLI and O. M. SREEDHARAN, *J. Mater. Sci. Lett.* **7** (1988) 714.
5. A. M. AZAD and O. M. SREEDHARAN, *ibid.* **8** (1989) 67.
6. R. PANKAJAVALLI and O. M. SREEDHARAN, *ibid.* **8** (1989) 225.
7. *Idem.*, *ibid.* **8** (1989) 697.
8. F. TOCI, A. SCHRUENKAMPER, M. CAMBINI and L. MANES, *Phys. C* **153/155** (1988) 838.
9. J. L. MacMANUS, D. J. FRAY and J. E. EVETTS, *Supercond. Sci. Technol.* **1** (1989) 291.
10. K. G. FRASE, E. G. LINIGER and D. A. CLARKE, *J. Amer. Ceram. Soc.* **70** (1987) C 204.
11. K. G. FRASE and D. A. CLARKE, *Adv. Ceram. Mater.* **2** (3B) (1987) 295 (special issue).
12. G. WANG, S.-J. WU, S. N. SONG, J. B. KETTERSON, L. D. MARKS, K. R. POEPPELMEIER and T. D. MASON, *ibid.* **2** (3B) (1987) 313.
13. R. S. ROTH, K. L. DAVIS and J. R. DENNIS, *ibid.* **2** (3B) (1987) 303.
14. D. M. DE LEEUW, C. A. H. A. MUTSAERS, C. LANGERIES, H. C. A. SMOORENBURG and P. J. ROMMERS, *Phys. C* **152** (1988) 39.
15. K. T. JACOB and Y. WASEDA, private communication.
16. Yu. D. TRETYAKOV, A. R. KAUL and N. V. MAKUKHIN, *J. Solid State Chem.* **17** (1976) 183.
17. A. M. AZAD and O. M. SREEDHARAN, *J. Appl. Electrochem.* **17** (1987) 949.
18. V. A. LEVITSKII, *J. Solid State Chem.* **25** (1978) 9.
19. G. H. RAO, J. K. LIANG and Z. Y. QIAO, *J. Less-Common Metals* **144** (1988) 215.

*Received 12 September 1989
and accepted 29 October 1990*